PAPER

Check for updates

Anaerobic biodegradation of citric acid in the presence of Ni and U at alkaline pH; impact on metal fate and speciation†

Natalie Byrd, [ID] *[a] Jonathan R. Lloyd, [ID] [a] Luke T. Townsend, [ID] [d] Joe S. Small,[a] Frank Taylor,[b] Heath Bagshaw,[c] Christopher Boothman,[a] Ilya Strashnov [ID] [e] and Katherine Morris*[a]

Citrate is a key decontaminant used in the nuclear industry and here we explore its biogeochemical fate in the presence of Ni^{2+} and $U(VI)O_2^{2+}$ under conditions relevant to low level radioactive waste (LLW) disposal. Anaerobic microcosm experiments were performed under nitrate- and sulfate-reducing conditions at between pH 9 and 10. Citrate (1 mM) was supplied as both an electron donor and a potential metal ion complexant. Incubation experiments with citrate, inoculated with nitrate- or sulfate-reducing microbial consortia, were challenged with three different concentrations of Ni: 0.01, 0.1 or 1 mM, or U: 0.005, 0.05, or 0.5 mM. The nitrate- and sulfate-reducing inocula were enriched from well characterised alkaline sediments obtained from high pH lime-workings. A multi-technique approach was adopted to characterise the aqueous geochemistry, solid phase mineralogy, and bacterial communities in each incubation system. In the 0.01 mM Ni systems citrate underwent full biodegradation under both nitrate and sulfate-reducing conditions in less than 15 days. In the sulfate-reducing experiments, 50% of the added 0.01 mM $Ni_{(aq)}$ was removed from solution and black solids formed; SEM and TEM analysis suggested that these were Ni-sulfides. For the higher Ni concentration incubations, no changes were observed in the nitrate-amended experiments. In the sulfate-amended experiments only citrate fermentation was observed, likely because elevated levels of Ni were toxic to nitrate- and sulfate-reducing bacteria in the inocula. Interestingly, although fermentative bacteria were key citrate degraders in the sulfate-amended experiments they did not dominate in the nitrate-amended experiments presumably due to competition from other microbes. In the U experiments, citrate degradation took place over 55 days in all systems except the 0.5 mM U/nitrate-amended incubations. In all U/sulfate-amended experiments, a dark-coloured precipitate formed and XAS analysis indicated that these solids contained reduced U(IV) with EXAFS suggesting that non-crystalline U(IV)−phosphate phases dominated. Microbial community analysis by 16S rRNA gene sequencing of endpoint samples identified fermenters and nitrate- and sulfate-reducing bacteria in the relevant incubations. Overall, findings suggest microbial degradation of citrate occurs under repository relevant conditions with Ni (at 0.01−0.1 mM) and U (at 0.005−0.5 mM) but with an inhibitory effect particularly at elevated Ni concentrations. Significantly, the work suggests that under anaerobic conditions relevant to LLW disposal, citrate undergoes biodegradation leading to the development of poorly soluble Ni sulfides and/or bioreduction of U(VI) to poorly soluble U(IV) phases. This suggests that both removal of citrate, and retention of Ni and U can occur in these environments and this information can be used to further inform development of safety cases for radioactive waste disposal.

[a]Research Centre for Radwaste Disposal and Williamson Research Centre, Department of Earth and Environmental Sciences, The University of Manchester, Manchester M13 9PL, UK. E-mail: katherine.morris@manchester.ac.uk

[b]Nuclear Waste Services, Pelham House, Seascale, Cumbria CA20 1DB, UK

[c]School of Engineering, The University of Liverpool, Liverpool, L69 3GQ, UK

[d]NucleUS Immobilisation Science Laboratory, Department of Materials Science and Engineering, The University of Sheffield, Sheffield, UK

[e]Department of Chemistry, University of Manchester, UK

† Electronic supplementary information (ESI) available. See DOI: https://doi.org/10.1039/d3va00061c

Environmental significance

Citrate, a naturally ubiquitous ligand, is a key decontaminant in the nuclear industry and is abundant in low level radioactive waste (LLW). Citrate complexation may promote contaminant metal/radionuclide migration in the environment; even at alkaline pH levels expected in cementitious LLW repositories. Understanding potential biodegradation mechanisms of citrate under LLW disposal conditions, where contaminant species (*e.g.* U, Ni) are present, is important to predict the impacts of citrate in wastes and to inform development of safety cases for LLW disposal. This work shows anaerobic citrate biodegradation at elevated pH, when Ni or U(VI) are present, leading to the development of poorly soluble Ni and U(IV) phases. Overall, findings directly inform the safety case for the UK's LLW repository and are relevant to other cementitious waste repositories worldwide.

Introduction

A key challenge in low level radioactive waste (LLW) management is to understand and predict the potential migration of metal contaminants, such as Ni and U, from the wastes. Radioactive waste management design aims to mitigate contaminant migration[1] typically by generating a localised anaerobic, high pH, reducing near-field environment post closure.[2–4] Here, the solubility and transport of metals may be affected by organic ligands within wastes.[5–9] Candidate organic ligands from decommissioning activities (citrate, oxalate, nitrilotriacetic acid [NTA] and ethylenediaminetetraacetic acid [EDTA]) can affect metal solubility even at alkaline pH, through the formation of metal–ligand complexes.[10–13] In particular, citrate may be present within typical LLW in significant quantities from nuclear decontamination operations.[14–16]

Citric acid (2-hydroxy-1,2,3-propanetricarboxylic acid, $C_6H_8O_7$) is a naturally ubiquitous and widely utilised molecule.[17–19] In the nuclear industry it is used as a decontaminant due to its behaviour as a multidentate ligand. It forms aqueous complexes *via* its hydroxyl and/or carboxylate groups with key radioactive species including Ni and U.[20–23] Metal–citrate complexes are considered relatively mobile in the environment[24–30] and an understanding of potential biodegradation mechanisms of citrate under LLW disposal conditions, where U and Ni are present is important to predict the impacts of using citrate as a decontaminant in nuclear decommissioning. Citrate can be utilised as an electron donor in a range of engineered and natural environments.[31–41] Recently, under alkaline conditions representative of a cementitious repository, citrate was shown to be an effective electron donor in support of anaerobic metabolism.[16] Furthermore, experiments showed that Fe(III)–citrate complexation may enhance the extent of high pH (pH 11.7) Fe(III)-bioreduction.[16]

In the current work, we explore the fate of both Ni^{2+} and $U(VI)O_2^{2+}$ in citrate biodegradation experiments as they are significant contaminants in many radioactive wastes.[9] Here, [63]Ni (half-life ~100 years) is present from neutron capture (by [62]Ni) and stable nickel is present from its use in *e.g.* corrosion resistant alloys.[42,43] In addition, U is typically the most significant radionuclide by mass in radioactive wastes including LLW.[9,44–47] The environmental mobility of U is influenced by its speciation and oxidation state at neutral to mildly alkaline pH. Relatively soluble $U(VI)_{(aq)}$ species can be (bio)reduced to poorly soluble U(IV), a key mechanism in promoting U immobilisation, including at elevated pH.[48,49] By contrast, Ni is not typically redox active, but is prone to immobilisation *via* the

precipitation of insoluble mineral phases, *e.g.* with sulfide or phosphate.[50,51]

At near-neutral pH, biodegradation of a range of metal–citrate complexes, including U, Pu, Eu, Fe(III), Ni, Co, Zn, Al, Cd, and Cu have been examined under both aerobic and anaerobic conditions.[7,20,21,32,52–58] Under these conditions, it was reported that biodegradation of metal–citrate complexes was dependant on the complex formed. Authors of this work suggested that tridentate complexes involving the hydroxyl group of the citrate ligand were recalcitrant to biodegradation, whilst bidentate complexes involving only the carboxylate groups were biodegradable.[20,59,60] The recalcitrance of tridentate complexes to biodegradation was attributed to their limited uptake into the cell, however potential U toxicity was not ruled out/discussed.[20,53,61]

Citrate is expected to form bidentate complexes with Ni(II) under circumneutral conditions, but under alkaline conditions tridentate complexation may be more favourable as the hydroxyl group may ionize to offer a further binding site.[23,62] Under neutral pH conditions, citrate forms bi-nuclear complexes with U(VI), *e.g.* $[(UO_2)_2(Cit)_2]^{2-}$, which are recalcitrant to biodegradation by *Pseudomonas fluorescens* under aerobic and denitrifying conditions.[20,53] Indeed, Francis *et al.*, suggested that the $[(UO_2)_2(Cit)_2]^{2-}$ species is stable up to pH 9.[53] However, thermodynamic modelling by Huang *et al.*, suggested that above pH 8, the hydroxyl complex $[(UO_2)_3(OH)_7]^{2-}$ would dominate[58] and this is supported by more recent thermodynamic data.[58,63,64] The study by Huang *et al.*, 1998 is one of the only studies to explore biodegradation of U–citrate complexes at alkaline pH (pH 8–9) experimentally and under aerobic conditions. The study showed the citrate biodegradation rate was higher at pH 8–9 than at pH 6–7.[52] Indeed, a range of metals, including Ni, Cu, Co, Tc, U, Th and Zn are shown to form complexes with citrate, and other organic ligands (*e.g.* EDTA, NTA, ISA).[12,65–69] Again, studies relating to biodegradation of these complexes under anaerobic, alkaline conditions are sparse.

Accordingly, further research regarding Ni/U/citrate speciation under elevated pH conditions is important to further understand Ni and U mobility in LLW disposal. Although LLW disposal facilities are expected to have a bulk pH of >11, waste form heterogeneity[70,71] and biogeochemical processes[16,72–74] may give rise to localised areas where pH is more neutral which may impact Ni/U/citrate speciation. In addition, evolution of the repository over time is expected to lead to more neutral pH.

In studies investigating microbial degradation of Ni– or U–citrate complexes, aerobic, citrate-degrading *Pseudomonas* cultures have been explored *e.g.*, *P. fluorescens* and *P.*

© 2023 The Author(s). Published by the Royal Society of Chemistry

Environ. Sci.: Adv., 2023, **2**, 1196–1209 | **1197**

alcaliphila.[52,62] In Ni–citrate degradation experiments with *P. fluorescens* and *P. alcaliphila*, partial degradation of bidentate [Ni(Cit)]$^-$ was observed[52,60,75] and *P. aeruginosa* and *P. putida*, were shown to fully degrade citrate in the presence of the bidentate [Ni(Cit)]$^-$ complex.[62] In an experimental system with *P. aeruginosa*, a small amount of Ni was removed from solution as $Ni_3(PO_4)_2 \cdot 8H_2O$.[62]

Under anaerobic conditions, there is a paucity of information on the biodegradation of Ni–citrate complexes, especially at alkaline pH. Qian *et al.*, found that a sulfate-reducing culture was able to degrade Ni–citrate at pH 6.8 to form nickel sulfide phases.[76] In addition, other disposal relevant organic Ni complexes, such as with isosaccharinic acid (ISA), a key degradation product of alkaline cellulose hydrolysis in ILW, have been shown to be degraded anaerobically at neutral pH and again, insoluble nickel sulfide phases were formed.[51]

Biodegradation of U(VI)–citrate complexes has been studied in pure culture using isolates of *Acinetobacter calcoaceticus*, *Citrobacter freundii*, *Pseudomonas stutzeri*, *P. aeruginosa*, *P. fluorescens* and *P. putida* under aerobic and denitrifying conditions at neutral pH and here, the U(VI)–citrate complex was not degraded.[20,53,58] Under anaerobic conditions, U(VI)–citrate was reduced to soluble U(IV)–citrate which implied that citrate complexed to U(VI) was not metabolised and overall reducing conditions in the presence of citrate did not favour precipitation of U(IV) minerals.[53] U(VI)–citrate and Ni–citrate systems are poorly explored under alkaline, anaerobic conditions, or using a mixed microbial culture despite their relevance to radioactive waste disposal. Here, citrate has the potential to behave as either a complexant to enhance metal solubility or an electron donor in support of nitrate, sulfate or U(VI) bioreduction, which may promote immobilisation *via* the formation of poorly soluble U(IV) species (*via* bioreduction) or by metal biomineralisation with metabolites (*e.g.* with sulfides from sulfate reduction). The aim of this study was to explore the anaerobic speciation and biogeochemical fate of Ni/U/citrate complexes at alkaline pH using mixed bacterial cultures enriched from alkaline impacted sediments. Throughout, we used a multi technique approach to understand the fate of citrate, nickel and uranium in these systems in order to further inform understanding of their biogeochemical fate in low level wastes. More broadly, this work can be used to inform bioremediation strategies for sites where radioactive waste is present and/or has led to near-surface contamination plumes.[77–80]

Methodology

Anaerobic enrichment experiments, under nitrate- and sulfate-reducing conditions were set up to explore biogeochemical fate of Ni/citrate or U/citrate at pH 9–10. During experiments, changes in geochemistry, mineralogy and microbiology were monitored. Geochemical modelling using PHREEQC,[81] with the ThermoChimie database (version 11a[64]), was used to support data interpretation (all modelling data are available in the ESI†). All aqueous reagents were filter sterilised prior to use. Concentrations of citrate and metals were selected to be representative of levels expected in a heterogeneous LLW repository.[3]

Sediment inoculum for primary enrichment cultures

Sediment was collected from a high pH site in Harpur Hill, Derbyshire, UK. The site is a well characterized legacy lime works; sediments have elevated pH and are Ca-rich and the geomicrobiology is considered representative of a high pH, cementitious repository.[73,82]

Primary enrichment cultures

Citrate oxidising cultures were enriched from the Harpur Hill sediment under nitrate- and sulfate-reducing conditions at pH 9. The primary enrichments contained 5 g of sediment, 100 mL minimal medium (9.4 mM NH_4Cl, 4.3 mM K_2HPO_4, 4 mM $NaHCO_3$, 10 mL L^{-1} vitamin and mineral mix[83]), 5 mM of trisodium citrate ($Na_3C_6H_5O_7$) as the sole carbon source and electron donor, and either $NaNO_3$ (30 mM) or Na_2SO_4 (15 mM) as the electron acceptor. The pH was adjusted to pH 9 using NaOH and inoculations were performed anaerobically. Under both nitrate- and sulfate-reducing conditions, stable enrichment cultures were obtained by transferring a 1% v/v inoculum from primary enrichments into fresh, heat-sterilized medium. Typically, at least 5 subcultures were performed prior to running Ni/U experiments. The nitrate-reducing cultures were transferred into minimal medium with 5 mM citrate and 30 mM nitrate.[83] The sulfate-reducing cultures were transferred into modified Postgate C medium with 5 mM citrate (no other organic electron donors included) and 30 mM sulfate.[84]

Nickel experiments

Preparation of Ni–citrate media. Ni–citrate medium was prepared for nitrate- and sulfate-reducing experiments at 0.01, 0.1 or 1 mM of Ni. These are referred to throughout as 'low', 'middle', or 'high' Ni systems.

Nitrate-reducing experiments

Three batches of minimal medium[83] were prepared. To each, 1 mM trisodium citrate ($Na_3C_6H_5O_7$) and 10 mM $NaNO_3$ were added. A stock solution (1 M Ni^{2+} in pH 3 HCl) was then added to target final Ni concentrations of 0.01, 0.1 or 1 mM and then pH was re-adjusted to pH 9–10 using NaOH. Experiments were then set up in 100 mL serum bottles under N_2 using aseptic technique, and in triplicate. After equilibration for 24 hours, bottles were sampled to monitor the initial solution chemistry prior to microbial inoculation. The bottles were then inoculated using 1% v/v of the nitrate-reducing culture obtained from the primary enrichments, stored at 20 °C in the dark and periodically sampled under anaerobic, aseptic conditions. Parallel, sterile controls without microbial inoculum were also set up.

Sulfate-reducing experiments

The sulfate-reducing experiments were set up in the same way as the nitrate-reducing systems, with two variations: (1) 10 mM sulfate was added instead of nitrate, (2) the sulfate-reducing enrichment culture (1% v/v) was used to inoculate the experiments.

| Paper | Environmental Science: Advances |

Uranium experiments

Uranium experiments were performed using washed resting cell cultures (late log phase) to prevent precipitation of uranium with components of bacterial growth medium (e.g., phosphate).

Preparation of U and citrate media

TRIS buffer (20 mM TRIS; pH 9–10) containing U and citrate was prepared for nitrate and sulfate reducing experiments. Three concentrations of U were added to experiment bottles in small volumes (<300 μL) using pH 3 UO_2^{2+} stock in HCl to target concentrations of 0.005, 0.05, or 0.5 mM, U(VI). After spiking, pH was adjusted to pH 9–10 for the experiments. These are referred to as 'low', 'middle' or 'high' U experiments throughout. Throughout, solutions were handled to minimise carbonate ingress.

Nitrate-reducing experiments

For the nitrate-reducing systems, 1 mM trisodium citrate ($Na_3C_6H_5O_7$), 10 mM $NaNO_3$ and U(VI) spike were added to give a U(VI) concentration of 0.005, 0.05, or 0.5 mM. Experiments were run in 50 mL glass serum bottles in triplicate. A nitrate-reducing culture (inoculated using the same enrichment culture used in the Ni experiments) was used to grow cells to late exponential phase. These cells were collected by centrifugation, washed three times in anaerobic TRIS buffer (20 mM, pH 9–10) and this resting cell culture was added to each 50 mL bottle to give each a final $OD_{600} = 0.2$. Parallel sterile controls (with heat-sterilised cells, as sorption controls) were also set up.

Sulfate-reducing experiments

Sulfate-reducing experiments were set up in the same way as the U(VI)-supplemented nitrate-reducing experiments, with two exceptions: (1) 10 mM Na_2SO_4 was added instead of $NaNO_3$; (2) a washed sulfate-reducing cell culture grown in Postgate C medium,[84] was added to give final $OD_{600} = 0.2$ in each bottle.

Solution chemistry

The pH was measured using a Mettler Toledo SevenCompact digital meter fitted with a calibrated Fisherbrand FB68801 electrode. Concentrations of anionic species (nitrate, sulfate, citrate, and volatile fatty acids) were measured by capillary anion exchange chromatography (IC) using a Dionex ICS5000. The lower limit of detection for citrate was 0.002 mM. Total aqueous Ni and U concentrations were measured on centrifuged and acidified samples (14 800g, 10 min; 2% HNO_3) using inductively coupled plasma mass-spectrometry (ICP-MS; Agilent 7500cx).

Electrospray ionisation mass spectrometry was used to examine Ni and citrate speciation at the start and end of select experiments (Thermo Q-exactive, Orbitrap mass analyser, attached to a Thermo Ultimate 3000 high performance liquid chromatography (HPLC)). Electrospray ionization was performed in both positive and negative polarity modes. The HPLC used an isocratic flow of 100% methanol for the mobile phase.

Solid phase analyses

Microscopy. Precipitates that formed in low Ni (0.01 mM) and low U (0.005 mM) sulfate-reducing systems were analysed by scanning electron microscopy (SEM) and transition electron microscopy (TEM). After centrifugation, (14 800g, 10 minutes) solids underwent a fixing, dehydration, and dilution protocol, using glutaraldehyde and ethanol, to preserve biological structures. Preserved samples for SEM were drop-cast onto an aluminium pin stub (Zeiss, Ø12.7 mm top), dried anaerobically and gold coated before imaging on a FEI Quanta 650 FEG instrument operating at 15 kV in high vacuum mode (10^5 to 10^{-6} mbar). Energy dispersive X-ray analysis (EDS) was performed using the EDAX Gemini EDS system. Samples from the Ni experiments were also analysed by TEM (JEOL 2100+ TEM). Samples were drop cast onto a gold grid with a holey carbon film and dried anaerobically. TEM images were captured using a Gatan RIO digital camera. EDS was obtained using an Oxford Instruments Xmax 65T Detector (65 mm window size); data collection and analysis was performed using Oxford Aztec Energy software.

Spectroscopic analysis

Solid samples were analysed by X-ray absorption spectroscopy (XAS) on beamline B18 at the Diamond Light Source, Harwell, UK from the low (0.005 mM; XANES and EXAFS) and middle (0.05 mM; XANES only) U experiments. Samples were centrifuged and the resultant solids dried in an oxygen free glove box and diluted by mixing with cellulose to target a final U concentration of 1% w/w. Sample pellets were pressed under N_2 and mounted on a sample holder and stored under a N_2 atmosphere at −80 °C until analysis. XAS data were obtained at the Diamond Light Source on B18 using the U L_{III} edge in transmission or fluorescence mode with a Ge detector. The Athena and Artemis (with FEFF6) software was used for fitting and data reduction.

Microbial community analysis

DNA extraction. DNA was extracted from 200 μL of homogenised slurry using a DNeasy PowerSoil Pro Kit (Qiagen, Manchester, U.K) at the start and end points in all systems.

16S rRNA gene sequencing. Sequencing of PCR amplicons of 16S rRNA genes were conducted with the Illumina MiSeq platform (Illumina, San Diego, CA, USA) targeting the V4 hyper variable region (forward primer, 515F, 5′-GTGY-CAGCMGCCGCGGTAA-3′; reverse primer, 806R, 5′-GGAC-TACHVGGGTWTCTAAT-3′) for 2 × 250-bp paired-end sequencing (Illumina[85,86]). PCR amplification was performed using Roche FastStart High Fidelity PCR System (Roche Diagnostics Ltd, Burgess Hill, UK) in 50 μL reactions under the following conditions: initial denaturation at 95 °C for 2 min, followed by 36 cycles of 95 °C for 30 s, 55 °C for 30 s, 72 °C for 1 min, and a final extension step of 5 min at 72 °C. The PCR products were purified and normalised to ~20 ng each using the SequalPrep Normalization Kit (Fisher Scientific). The PCR amplicons from all samples were pooled in equimolar ratios.

The run was performed using a 4.5 pM sample library spiked with 4.5pM PhiX to a final concentration of 12% following the method of Schloss and Kozich.[87]

Post-sequencing analysis

Raw sequences were divided into samples by barcodes (up to one mismatch was permitted) using a sequencing pipeline. Quality control and trimming was performed using Cutadapt4, FastQC5, and Sickle6. MiSeq error correction was performed using SPADes7. Forward and reverse reads were incorporated into full-length sequences with Pandaseq8, and chimeras were removed using ChimeraSlayer9. OTU's were generated for the 16S rRNA gene sequences with UPARSE10. OTUs were classified by Usearch11 at the 97% similarity level, and singletons were removed. Rarefaction analysis was conducted using the original detected OTUs in Qiime12. The taxonomic assignment was performed by the RDP naïve Bayesian classifier version 2.2 13, used in combination with the Silva SSU 132 ribosomal RNA gene database 14. The OTU tables were rarefied to the sample containing the lowest number of sequences, all samples having less than 5000 sequences were removed from analyses prior to the rarefaction step. The step size used was 2000 and 10 iterations were performed at each step.

Results and discussion

Anaerobic enrichment experiments were used to investigate the biogeochemical fate of Ni, U and citrate at alkaline pH. Three sets of experiments, using 0.01, 0.1 or 1 mM Ni^{2+} or 0.005, 0.05, or 0.5 mM $U(VI)O_2^{2+}$, were performed under nitrate- and sulfate-reducing conditions.

Nitrate-reducing experiments

Ni/nitrate-reducing conditions. In the inoculated low Ni (0.01 mM) experiment, all added citrate (0.8 ± 0.5 mM) was removed from solution within 15 days, and the pH fell from pH 9.1 to pH 8.6 (1A–D). No organic degradation products such as volatile fatty acids (VFAs), were detected by IC in any of the inoculated samples. Although other products could include alcohols or H_2, data here suggested citrate had been completely oxidised to CO_2. Indeed, alongside citrate removal, the nitrate concentration decreased from 10.2 mM to 3.8 mM (6.4 ± 0.03 mM) over 15 days and stoichiometric production of 6.6 ± 1.2 mM nitrite was measured,[88] consistent with past work from high pH citrate-oxidising/nitrate-reducing microcosms.[16] After the initial 15 day incubation, there was no further denitrification over the remaining experimental incubation (experimental end point 160 days) presumably due to citrate depletion.

Geochemical modelling (Fig. S5†) of the 0.01 mM Ni/1 mM citrate system at $t = 0$ predicted that 91% of the Ni was present as $[Ni(Cit)]^-$ and 9% as the $[Ni(Cit)_2]^{4-}$ species. The ESI-MS analysis for the $t = 0$ aqueous sample (Fig. S7†), showed a peak at 246.9384 m/z consistent with the $[Ni(Cit)]^-$ species (246.9389 g mol^{-1}). This peak was absent in the 162 day sample at the experimental end point indicating that, consistent with the bulk citrate

Fig. 1 Aqueous geochemistry data for the Ni and U nitrate-reducing experiments. Top – low (0.01 mM) Ni, nitrate-reducing experiment, Bottom – low and middle U, nitrate-reducing experiments. Columns from left to right are: pH (A, E, I), citrate concentration (B, F, J), nitrate/nitrite concentration (C, G, K) and nickel/uranium concentration (D, H, L). Green lines – low Ni/U systems, blue lines – middle U experiments, dashed black lines – sterile control, grey line (Ni only) – no citrate control. Error bars represent 1σ of the triplicate samples.

measurements, $[Ni(Cit)]^-$ had been degraded. Interestingly, there was no evidence for the $[Ni(Cit)_2]^{4-}$ species (expected at 439.9737 g mol^{-1}) in the 0 day time point in the ESI-MS, which was predicted at low levels in the thermodynamic modelling and has been suggested as a significant species at pH 9.[60,89]

Despite the removal of $[Ni(Cit)]^-$ (in the low Ni systems) during incubation, and as evidenced in the ESI data, Ni remained soluble throughout incubation (Fig. 1D). Here, geochemical modelling predicted that in the end-point experiment, where HCO_3^- had presumably grown in from citrate degradation (4.8 mM; eqn (S1)†,[16]), Ni^{2+} would be a significant aqueous species, and that $NiCO_3$ and $Ni(OH)_2$ would be oversaturated (Fig. S6†). Interestingly, there was no removal of Ni in the experimental endpoints or the controls, suggesting that the Ni^{2+} (aq) species dominated in the nitrate-reducing incubation end points.

Overall, the data suggest that in nitrate-reducing systems with low Ni concentrations, Ni is soluble initially as Ni–citrate and as degradation of the bioavailable Ni–citrate complex occurs, it is likely present as the Ni^{2+} aqueous species. In the middle and high Ni inoculations there were no changes in pH, Ni, citrate and nitrate concentrations despite the presence of citrate (Fig. 1A–D, S1 & S5, Table S1†). This suggests the elevated Ni concentrations were toxic.[90–92]

U/nitrate reducing systems

Under nitrate-reducing conditions, the citrate concentrations fell in the low and middle U systems with 100% citrate removal (0.7 ± 0.1 mM) in the low U system, and 30% citrate removal (0.2 ± 0.1 mM) in the middle U system by day 15 (Fig. 1F and J). At the same time, reduction of nitrate to nitrite was seen in both systems (Fig. 1G and K). In the inoculated low U system, the solution pH decreased from pH 9.8 to 9.1 (Fig. 1E), whilst no significant pH change was measured in the middle U system (Fig. 1I). As observed in the Ni experiments, no VFAs were detected in either system, suggesting citrate was fully oxidised to CO_2 in inoculated systems consistent with solution acidification associated with CO_2 dissolution into solution.

Interestingly, uranium concentrations remained constant throughout the nitrate-reducing experiment confirming citrate-driven nitrate reduction did not affect U(vi) solubility (Fig. 1H and L). This is consistent with the geochemical modelling of the starting solution which predicted a small fraction (0.03–0.1%) of the added U would form citrate complexes, and that, in the absence of carbonate, aqueous U(vi) was present as hydroxide species (including $[UO_2(OH)_3]^-$, and $[(UO_2)_3(OH)_7]^-$) with the vast majority of citrate present as the free citrate $[Cit]^{3-}$ species (Fig. S5 and Table S1†). Modelling of the U solid phases at the initial time point predicted that in the absence of carbonate, there was oversaturation of mineral phases including clarkeite, metaschoepite and Na-compreignacite, in contrast to the aqueous data obtained (Fig. 4C, F and I). The increased solubility of U in some experiments compared to the thermodynamic modelling at the initial timepoint may be explained by either the dynamic nature of the experiments or in the absence of extensive U–citrate complexation, may be due to

complexation by residual carbonate in solution. Geochemical modelling data for the end-point solutions in these nitrate-reducing systems, after citrate degradation to HCO_3^-, suggested that U(vi) would be present as aqueous U(vi)–carbonate species and that likely solid U phases (e.g., metaschoepite, clarkeite, rutherfordine and $UO_2(OH)_2$), were undersaturated (Fig. S6†).

Geochemical modelling data for the end-point solutions in these nitrate-reducing systems, after citrate degradation to HCO_3^-, suggested that U(vi) would be present as aqueous U(vi)–carbonate species and that likely solid U phases (e.g., metaschoepite, clarkeite, rutherfordine and $UO_2(OH)_2$), were undersaturated (Fig. S6†). Again, elevated U levels in the middle and high U experiments (0.05 mM, 0.5 mM) likely inhibited bacterial activity in the inoculum.[93,94] Indeed, in the high U incubations no changes in pH, or citrate and nitrate/nitrite concentration were observed, and, in middle U incubations only modest changes (e.g., 30% citrate removal and 11% nitrate reduction) were observed when compared to the low U system (Fig. 1I–L).

Overall, the data from these nitrate-reducing experiments showed rapid citrate biodegradation can occur at elevated pH under nitrate-reducing conditions when Ni and U are present at trace levels, however citrate biodegradation may be hindered by metal toxicity where elevated concentrations of these metals are present.

Sulfate-reducing experiments

Ni/sulfate-reducing systems. In the inoculated low Ni, sulfate-reducing experiment, essentially all the 1 mM added citrate was fully removed from solution by day 12 followed by ingrowth of acetate and formate to concentrations of 1.4 ± 0.1 mM and 0.6 ± 0.1 mM, respectively at 12 days (Fig. 2A and B). This is consistent with citrate fermentation to acetate and formate. After 42 days the formate had been removed from solution and all repeat bottles had black precipitates present suggesting sulfide formation. Further acetate removal was observed in two of the triplicate bottles by day 100; removal of 1.5 mM in bottle 1 and 0.5 mM in bottle 2 (Fig. 2B). Sulfate removal was noted in end point samples from all bottles in the microbially active low Ni experiments, although the extent of removal varied significantly between bottles; 1.6 mM (bottle 1), 1.0 mM (bottle 2), and 0.3 mM (bottle 3) (Fig. 3A). The extent of sulfate removal reflected the extent of electron donor depletion in each bottle (Fig. 2B and 3A).

In terms of Ni concentrations in solution, the average Ni removal for all bottles was 7.5 ± 2.0 μM (approximately 50% removal: Fig. 2C). In individual incubations the extent of Ni removal was greatest in bottles where sulfate removal was greatest with bottle 1 (0.009 mM) > bottle 2 (0.006 mM) > bottle 3 (0.004 mM; Fig. 3A). In terms of Ni solution speciation, ESI-MS confirmed that the Ni was complexed as a $[Ni(Cit)]^-$ species in the day 0 samples and that by day 100 this species was no longer present (consistent with citrate degradation). In this experiment the dominant Ni species was predicted to be $Ni(CO_3)$ (Fig. S6†), however no Ni–carbonate species were detected by ESI-MS

Fig. 2 Data showing the aqueous geochemistry for the Ni, sulfate-reducing experiments. Top (green) – low (0.01 mM) Ni, Bottom (blue) – middle Ni (0.1 mM). Columns from left to right are: citrate concentration (A, D), VFA concentration (B, E), nickel concentration (C, F). Green lines – inoculated individual bottles from low Ni systems (individual bottles are plotted as there was high variability between bottles in the triplicate set), blue lines – inoculated average measurement from middle Ni experiments, dashed grey lines – sterile control. Error bars represent 1σ of the triplicate samples.

analysis so presumably the dominant Ni(aq) species was Ni^{2+} (Fig. S6 and S8†).

At day 100 the removal of 7.5 ± 2 μM Ni from solution was accompanied by the formation of a black precipitate by day 42 consistent with formation of a Ni-sulfide phase.[51,95,96] SEM images from the sample at 100 days showed amorphous material, presumably biomass, and EDS analysis of these regions revealed the co-location of Ni and S (Fig. S10†). High resolution TEM imaging with corresponding EDS (Fig. S11†) also confirmed the co-location of Ni and S, and selected area diffraction analysis suggested that the precipitate was amorphous. Overall these data suggest an amorphous NiS-like precipitate was forming.

In the inoculated middle Ni, sulfate-reducing systems, citrate degradation occurred but at a slower rate than the low Ni-sulfate experiment. Significant but not complete citrate removal was observed in these systems and by day 100, 0.07 ± 0.01 mM citrate remained in solution. Citrate again was fermented to acetate and formate, which peaked at 1.4 ± 0.09 mM and 0.4 ± 0.2 mM, at day 100 and 40 respectively (Fig. 2D and E). Interestingly, there was no evidence, from blackening or sulfate removal, for the development of sulfate reduction in the middle Ni concentration experiment (Fig. 3B). Here, after their increase with time, acetate and formate did not degrade further suggesting progression to sulfate reduction was inhibited. Furthermore, ESI-MS confirmed that, contrary to the low Ni experiment, the $[Ni(Cit)]^-$ species remained dominant in solution over 100 days (Fig. S9†) consistent incomplete citrate degradation (Fig. 2D) and the full retention of complexed Ni in

solution (Fig. 3F). There were no observed biogeochemical changes in the high Ni systems, presumably due to Ni toxicity (Fig. S2† (ref. 90–92)).

Overall, for the low Ni experiments, the geochemical and microscopy data indicated that Ni–citrate complexes were degraded at pH 9. The data suggested a two-step mechanism where citrate was fermented to acetate and formate, which were then used to support sulfate reduction to variable degrees in the different bottles. Following sulfate reduction in the low Ni system, ESI-MS indicated Ni–citrate complexes were no longer present with aqueous phase analysis showing modest Ni^{2+} removal (50%) and solid phase characterisation suggesting amorphous Ni–sulfides had formed. By contrast, although significant fermentation of citrate to formate and acetate was observed in the middle Ni system, the elevated Ni concentration apparently inhibited sulfate reduction. Interestingly, this suggested in the 0.1 mM Ni experiment, that citrate fermentation was possible, but anaerobic sulfate reduction was inhibited. Here, ESI-MS analysis of the middle Ni solution phase at 100 days confirmed that the $[Ni(Cit)]^-$ complex was still present and ICP-MS showed all Ni remained soluble. Geochemical modelling of the low Ni system with 1 mM sulfide (as observed) and 0.01 mM citrate (enough to complex all added Ni), predicted oversaturation of insoluble Ni–sulfide phases would occur consistent with partial removal to nickel sulphides as observed in TEM (Table S2†).

It is interesting that fermentation occurs in sulfate-reducing systems but not in the nitrate reducing systems. At low Ni levels (0.01 mM), nitrate reducing bacteria may have outcompeted
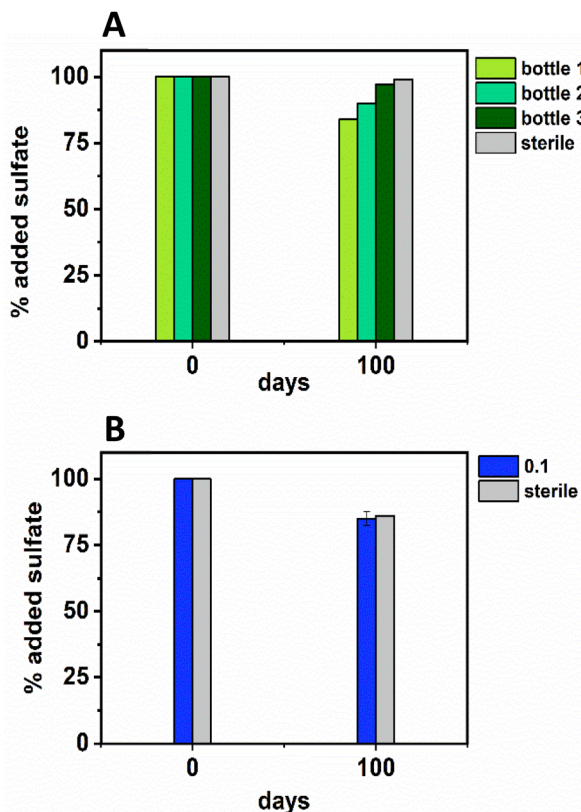
Fig. 3 Sulfate removal data from the low Ni (0.01 mM; top, A, in green) and middle Ni (0.1 mM; bottom, B, in blue) showing the percentage removal by the experimental end point at day 100. For the low Ni experiment (green) each bottle of the triplicate is plotted (due to high variability in between bottles in the triplicate experiment), and, for the middle Ni experiment the average $\pm 1\sigma$ is plotted.

fermentative bacteria. Indeed, past work has demonstrated that nitrate reducers can outcompete fermentative bacteria, particularly where C : N ratios are low as they are in the current study.[97–100] At higher Ni levels metal toxicity presumably inhibited microbial activity.

U/sulfate-reducing conditions

The inoculated low and middle U, sulfate-reducing experiments showed rapid and complete oxidation of citrate in the first 6 days of the experiment. After this, substantial acetate ingrowth was observed; 1.6 ± 0.06 mM by day 43 (low U, Fig. 4A), and 1.7 ± 0.05 mM by day 15 (middle U, Fig. 4D). These levels were then maintained up to day 55. Additionally, by day 15 formate ingrowth of 0.12 ± 0.01 mM (low U) and 0.10 ± 0.01 mM (middle U) occurred, and formate was then below the level of detection by day 55 in the middle U system. Partial and variable citrate removal (0.06–0.13 mM) was observed at 55 days in the high U triplicate experiment. After day 15 this was accompanied by production of 0.1 ± 0.01 mM acetate (no formate was detected in these samples), and these levels were maintained up to day 55 (Fig. 4G).

In the low (0.005 mM) and middle (0.05 mM) U incubations, dark precipitates had formed by day 12. Here, aqueous phase

analysis of the low and middle U systems showed near complete removal of U from solution by day 15 (Fig. 4C and F). In the high U system, dark precipitates had formed by day 43 and by day 55, there was between 40–69% U removal (Fig. 4I). Interestingly, there was no measurable sulfate removal in these incubations over the 55 day experiment (Fig. 4B, E and H) and this suggests direct enzymatic U(VI) reduction took place, rather than a mechanism coupled to sulfate-reduction. The uranium precipitates were further analysed in the low and middle U systems by X-ray absorption spectroscopy.

Analysis of the U L_{III} edge XANES spectra (Fig. 5) using U(VI)–uranyl and U(IV)–uraninite standards, suggested that significant reduction from U(VI) to U(IV) had occurred in both samples (Fig. 5). EXAFS data were also available for the solids from the low concentration U experiment. Here, the relevant published literature for biogenic non-crystalline U(IV) and nanoparticulate uraninite was used to inform the best fit model for the EXAFS spectra[101–104] (Fig. 5, Table S3 and S4†). Fitting initially considered biogenic uraninite and this provided a poor fit (R-factor > 0.02; Table S4†). An improved fit was achieved with a split oxygen shell of 4.5 O backscatterers at 2.31 Å and 3.5 O backscatterers at 2.49 Å, 1.5 P backscatterers at 3.14 Å, 1 P backscatter at 3.64, and 2.5 U backscatterers at 3.84 Å which was statistically significant (Table S3†). This fit suggests contributions from biogenic non-crystalline U(IV) coordinated by phosphate groups presumably present in the cell biomass in the experiment as observed in past work.[101–103,105–109]

16S rRNA gene sequencing. The microbial community composition in experiments was assessed using 16S rRNA gene sequencing with the illumina® MiSeq™ platform. The inocula (citrate-oxidising/nitrate- or sulfate-reducing cultures) used in these experiments were enriched under nitrate- or sulfate-reducing conditions from pH 10 sediment microcosms which contained sediments from a legacy lime working site.[73,82] The DNA extracted directly from the sediment was sequenced previously, and a diverse community with 562 operational taxonomic units (OTUs) was detected.[16] The enrichment cultures used to inoculate the Ni-supplemented experiments, and to grow resting cells for the U experiments, were less diverse and contained 41 OTUs (nitrate-reducing), and 53 OTUs (sulfate-reducing). Here, only starting enrichment-inocula and endpoint samples from experiments where biogeochemical changes were observed were sequenced. For the nitrate-reducing systems this was the low Ni and U experiments, and for the sulfate-reducing systems this was the low and middle Ni experiments and the low, middle and high U experiments.

Nitrate-reducing experiments

At the phylogenetic class level, the initial nitrate-reducing enrichment culture was dominated by Gammaproteobacteria (87%), Alphaproteobacteria (7%) and Bacilli (6%). In the low Ni experiment, after 160 days incubation the community had a relative increase in Alphaproteobacteria (26%) and Bacilli (31%), which grew at the expense of the Gammaproteobacteria (40%). At the genus level, in the nitrate-reducing enrichment culture *Pseudomonas* was dominant (54.4% of sequences),

Fig. 4 Aqueous organic acid (A, D, G), sulfate (B, E, H) and U concentration (C, F, I), data from the sulfate-reducing experiment with added U concentration of 0.005 mM U (top row, green), 0.05 mM U (middle row, blue) and 1 mM U (bottom row, pink). For the 0.5 mM U experiment only 2 out of 3 bottles in the triplicate are shown as the third bottle did not show geochemical changes. Presumably culture heterogeneity/toxicity in these "extreme" (i.e., alkaline pH) systems is impacting on the different experiment bottles.

Fig. 5 U L_{III}-edge spectra for solids from the low (0.005 mM) U and middle (0.05 mM) U samples. These samples are compared with U(VI) (aqueous U(VI)–triscarbonate) and U(IV) (uraninite) standards taken from previous work (Roberts et al., 2017; Townsend et al., 2020). Right: U L_{III}-edge XAS spectra for NB1. Top – k3-weighted EXAFS. Bottom – Fourier transform of k3-weighted EXAFS, using a Hanning window function.

followed by *Achromobacter* (18.7%); both genera have citrate-oxidising and nitrate-reducing members. In the Ni experiment, the endpoint sample (T_{160}) had substantial ingrowth from the genera *Anaerobacillus* (29.4%) and *Bosea* ('*Bosea 1*' on Fig. 6; 12.8%), and again, some members of both genera reduce nitrate and oxidise citrate (e.g.[37,110,111]). Interestingly, at the species level, a close match for the *Anaerobacillus* sequence was *Anaerobacillus alkaliphilus* (99.6% match). This organism is reported to encode various proteins that may contribute towards Ni resistance/tolerance e.g. several metal ABC transporter proteins (e.g. NCBI Reference Sequence WP_129076357;[112]). In the U experiments a resting cell culture was used and this was grown using the same enrichment culture inoculum used to inoculate the Ni experiments. In turn, the community structure in the low U, day 15 samples reflected the initial enrichment culture inoculum: Gammaproteobacteria (61%), Alphaproteobacteria (34%) and Bacilli (5%). *Pseudomonas* was also the dominant genus in the endpoint sample from the U-experiment (60%).

Sulfate-reducing experiment

At the phylogenetic class level the sulfate-reducing enrichment culture comprised mostly Bacilli (73%), Gammaproteobacteria (14%) and Clostridia (9%). The samples from the U-experiments, contained resting cells which were grown from

1204 | Environ. Sci.: Adv., 2023, **2**, 1196–1209

© 2023 The Author(s). Published by the Royal Society of Chemistry

Fig. 6 Data from 16S rRNA gene sequencing showing the microbial community, at genus-level, in end point samples from the (A) nitrate-reducing (B) sulfate-reducing experiments, in comparison to the initial enrichment culture inoculum. Where genus-level data could not be resolved, this is indicated by brackets *e.g.*, '(Prolixibacteraceae)'. Numbers in brackets *e.g.*, 'Bosea (1)' indicate significantly different gene sequences, presumably for different species.

the same sulfate-reducing enrichment culture that was used in the Ni experiments. In the endpoint samples from the U-experiments, cultures were similar to the starting inoculum; dominated by Bacilli (67–90%) and Clostridia (14%). In the 0.01 mM Ni supplemented incubations, communities changed over the duration of incubation and there was a substantial relative increase in Bacteroidia (18%), Gammaproteobacteria (33%) and Clostridia (24%). In the 0.1 mM Ni incubations, Bacilli were the dominant class in all samples (96%). Interestingly, in the 0.01 mM Ni experiments the genus level data showed increased diversity in the endpoint samples, although reasons for this remain unclear. In all other samples from sulfate-reducing experiments, diversity was constant or decreased following incubation with Ni or U (Fig. 6).

In the Ni experiment, the three most dominant genera were *Dechloromonas* (22%), *Trichococcus* (19%) and an unresolved genus of the order *Sphingobacteriales* (10%). Sulfate-reducing bacteria were identified in the low Ni experiment and in all U experiments. These were primarily affiliated with the genus *Desulfovibrio* which accounted for approximately 1–11% of the

communities. At the species level, the closest match to the *Desulfovibrio* (1) sequence (Fig. 6) was *Desulfovibrio mexicanus* (100% match), which is known to utilise acetate and formate as electron donors.[113] In addition, organisms affiliated with the sulfate-reducing genus *Desulfobulbus* were also identified in the 0.05 mM supplemented U experiment (3% of the community).

In the 0.1 mM Ni systems the samples were overwhelmingly dominated by the *Trichococcus* genus (97% of the community), and this organism was also dominant in all of the U systems (0.005 mM U – 60%, 0.05 mM U – 55%, and 0.5 mM U – 85% of the communities). This organism was also present to a lesser extent in the 0.01 mM Ni experiment (37%). Members of the genus *Trichococcus* are typically fermentative, and thus, the dominance of this genus supports the suggestion that citrate was initially fermented in all sulfate-reducing systems.[114]

Conclusions

Overall experiments show that robust citrate biodegradation took place in the presence of low levels of Ni and U, under

© 2023 The Author(s). Published by the Royal Society of Chemistry

Environ. Sci.: Adv., 2023, **2**, 1196–1209 | **1205**

conditions relevant to alkaline radioactive waste repository environments. In the Ni–citrate systems, anaerobic biodegradation of $[Ni(Cit)]^-$ at alkaline pH (pH 9) occurred under nitrate- and sulfate-reducing conditions when 0.01 mM Ni was present (Fig. 1 and 2). At higher metal loadings, growth of nitrate- and sulfate-reducing bacteria may be inhibited. This may be beneficial where negative impacts of microbial metabolism are observed for example, sulfate-reduction and its impact on corrosion.[115–118] In the sulfate reducing/0.01 mM Ni experiments, fermentation of citrate led to ingrowth of formate and acetate which then fuelled significant sulfate reduction (Fig. 2 and 3). Here, 50% of the added Ni (7.5 ± 2 μM) was immobilised under sulfate-reducing conditions as amorphous Ni–sulfide-like phases. Elevated Ni levels of 0.1- and 1 mM Ni were presumed to be toxic to both the nitrate- and sulfate-reducing cultures, except for members of the strictly fermentative genus *Trichococcus* in the 0.1 mM sulfate-reducing experiments (Fig. 2 and 6). Interestingly, ESI-MS showed the $[Ni(Cit)]^-$ complex did not degrade in the 0.1 mM Ni/sulfate-reducing experiments, even though significant, but not complete citrate removal was observed by IC (Fig. S8–S9,† 2). This suggests that sulfate-reducing bacteria were inhibited by toxicity from 0.1 mM Ni or the $[Ni(Cit)]^-$ complex. In turn, this impacted the end-state of this microcosm as NiS-like phases did not form and Ni remained largely soluble as the Ni–citrate complex.

Citrate biodegradation occurred in the presence of U under nitrate- and sulfate-reducing conditions, at alkaline pH (Fig. 1 and 3). In the nitrate-reducing system 0.5 mM U was toxic to the microbes over the experimental timescale. However, in the sulfate-reducing systems citrate removal was observed in all experiments, even when 0.5 mM U was present (Fig. 3). Importantly, in all sulfate-reducing systems citrate fermentation products (acetate & formate) likely supported enzymatic U(vi) reduction which led to reductive precipitation of a nanoparticulate U(iv)–phosphate phase likely formed through reaction with phosphate associated with the biomass in the experiment (Fig. 5). This study has demonstrated that at pH 9–10 under sulfate-reducing conditions bacteria can ferment citrate, a widely used decontaminant in the nuclear industry. The citrate fermentation products can then support sulfidation in low Ni systems to partially precipitate nickel sulfides and bioreduce U(vi) to form poorly soluble non-crystalline U(iv)–phosphates. Removal of citrate by biodegradation in wastes at high pH will eliminate the potential for radionuclide-citrate complexation, and the implied elevated solubility of radionuclides, notably Ni^{2+}, in radioactive waste disposal scenarios where citrate is present.

Author contributions

NB – conceptualization, methodology, investigation, data curation, formal analysis, visualisation, project administration, writing – original draft, writing – review & editing. JRL – conceptualization, methodology, writing – review & editing, resources, supervision, validation. LTT – XAS data curation and formal analysis, writing – review & editing. JSS – conceptualization, validation. FT – conceptualization, writing – review &

Conflicts of interest

The authors declare that this study received funding from Low Level Waste Repository Ltd. The funder had the following involvement with the study: conceptualization, writing – review & editing, supervision, funding acquisition, validation. The funder was not involved in the collection, analysis and interpretation of data, or, the decision to submit it for publication. FT was employed by company Low Level Waste Repository Ltd. The remaining authors declare that the research was conducted in the absence of any commercial or financial relationships that could be construed as a potential conflict of interest.

Acknowledgements

Notes and references

1 IAEA, *Iaea Ssr-5*, 2014, WS-R-1, 29.
2 U. R. Berner, *Waste Manag.*, 1992, **12**, 201–219.
3 LLW Repository Ltd., LLWR/ESC/R(11)10019
4 L. Duro, C. Domènech, M. Grivé, G. Roman-Ross, J. Bruno and K. Källström, *Appl. Geochem.*, 2014, **49**, 192–205.
5 D. Read, D. Ross and R. J. Sims, *J. Contam. Hydrol.*, 1998, **35**, 235–248.
6 L. R. Van Loon, M. A. Glaus and K. Vercammen, *Acta Chem. Scand.*, 1999, **53**, 235–240.
7 A. J. Francis, C. J. Dodge and J. B. Gillow, *Radiochim. Acta*, 2006, **94**, 731–737.
8 W. Hummel, *Monatshefte fur Chemie*, 2008, **139**, 459–480.
9 M. J. Keith-Roach, *Sci. Total Environ.*, 2008, **396**, 1–11.
10 M. Sutton, *Uranium solubility, speciation and complexation at high pH*, University of Loughborough, 1999.
11 N. D. M. Evans, S. A. Gascón, S. Vines and M. Felipe-Sotelo, *Mineral. Mag.*, 2012, **76**, 3425–3434.
12 M. Felipe-Sotelo, M. Edgar, T. Beattie, P. Warwick, N. D. M. Evans and D. Read, *J. Hazard. Mater.*, 2015, **300**, 553–560.

13 M. Felipe-Sotelo, J. Hinchliff, L. P. Field, A. E. Milodowski, J. D. Holt, S. E. Taylor and D. Read, *J. Hazard. Mater.*, 2016, **314**, 211–219.

14 R. Serne, A. Felmy and K. J. Cantrell, *Characterization of Radionuclide-Chelating Agent Complexes Found in Low-Level Radioactive Decontamination Waste*, Pacific Northwest National Laboratory, NUREG/CR-6124, PNL-8856, 1996.

15 IAEA, *Management of low and intermediate level radioactive wastes with regard to their chemical toxicity*, Vienna, 2002.

16 N. Byrd, J. R. Lloyd, J. Small, F. Taylor, H. Bagshaw, C. Boothman and K. Morris, *Front. Microbiol.*, 2021, **12**, 1–22.

17 H. A. Krebs, *Biochem. J.*, 1940, **34**, 460–463.

18 J. L. Pierre and I. Gautier-Luneau, *BioMetals*, 2000, **13**, 91–96.

19 R. Ciriminna, F. Meneguzzo, R. Delisi and M. Pagliaro, *Chem. Cent. J.*, 2017, **11**, 1–9.

20 A. J. Francis, C. J. Dodge and J. B. Gillow, *Nature*, 1992, **356**, 57–59.

21 S. C. Brooks, J. S. Herman, G. M. Hornberger and A. L. Mills, *J. Contam. Hydrol.*, 1998, **32**, 99–115.

22 A. Apelblat, *Citric Acid*, Springer International Publishing, Switzerland, 2014.

23 J. P. Glusker, *Acc. Chem. Res.*, 1980, **13**, 345–352.

24 U. Neubauer, G. Furrer, A. Kayser and R. Schulin, *Int. J. Phytorem.*, 2000, **2**, 353–368.

25 A. P. Schwab, D. S. Zhu and M. K. Banks, *Chemosphere*, 2008, **72**, 986–994.

26 L. Duquène, F. Tack, E. Meers, J. Baeten, J. Wannijn and H. Vandenhove, *Sci. Total Environ.*, 2008, **391**, 26–33.

27 I. F. Poulsen and H. C. B. Hansen, *Water. Air. Soil Pollut.*, 2000, **120**, 249–259.

28 N. U. Yamaguchi, A. C. Scheinost and D. L. Sparks, *Clays Clay Miner.*, 2002, **50**, 784–790.

29 A. P. Schwab, Y. He and M. K. Banks, *J. Environ. Eng.*, 2004, **130**, 1180–1187.

30 X. Liang, Y. Zang, Y. Xu, X. Tan, W. Hou, L. Wang and Y. Sun, *Colloids Surf., A*, 2013, **433**, 122–131.

31 M. J. C. Starrenburg and J. Hugenholtz, *Appl. Environ. Microbiol.*, 1991, **57**, 3535–3540.

32 A. J. Francis, C. J. Dodge, J. B. Gillow and H. W. Papenguth, *Environ. Sci. Technol.*, 2000, **34**, 2311–2317.

33 Y. V. Boltyanskaya, V. V. Kevbrin, A. M. Lysenko, T. V. Kolganova, T. P. Tourova, G. A. Osipov and T. N. Zhilina, *Microbiology*, 2007, **76**, 739–747.

34 K. K. Kim, L. Jin, H. C. Yang and S. T. Lee, *Int. J. Syst. Evol. Microbiol.*, 2007, **57**, 675–681.

35 X. W. Xu, Y. H. Wu, Z. Zhou, C. S. Wang, Y. G. Zhou, H. Bin Zhang, Y. Wang and M. Wu, *Int. J. Syst. Evol. Microbiol.*, 2007, **57**, 1619–1624.

36 S. Fox, N. Mozes, O. Lahav, N. Mirzoyan and A. Gross, *Water. Air. Soil Pollut.*, 2015, **226**, 134.

37 J. Switzer Blum, A. Burns Bindi, J. Buzzelli, J. F. Stolz and R. S. Oremland, *Arch. Microbiol.*, 1998, **171**, 19–30.

38 J. Switzer Blum, S. Hoeft McCann, S. Bennett, L. G. Miller, J. F. Stolz, B. Stoneburner, C. Saltikov and R. S. Oremland, *Geomicrobiol. J.*, 2016, **33**, 677–689.

39 H. Yang, P. Shao, T. Lu, J. Shen, D. Wang, Z. Xu and X. Yuan, *Int. J. Hydrogen Energy*, 2006, **31**, 1306–1313.

40 V. M. Gámez, R. Sierra-Alvarez, R. J. Waltz and J. A. Field, *Biodegradation*, 2009, **20**, 499–510.

41 A. J. M. Stams, J. Huisman, P. A. Garcia Encina and G. Muyzer, *Appl. Microbiol. Biotechnol.*, 2009, **83**, 957–963.

42 D. Féron, in *Nuclear Corrosion Science and Engineering*, ed. D. Féron, Woodhead Publishing, 2012, pp. 31–56.

43 C. A. C. Sequeira, D. S. P. Cardoso, L. Amaral, B. Šljukić and D. M. F. Santos, *Corros. Rev.*, 2016, **34**, 187–200.

44 H. S. Klapper, N. S. Zadorozne and R. B. Rebak, *Acta Metall. Sin.*, 2017, **30**, 296–305.

45 M. L. Carboneau and J. P. Adams, *National Low-Level Waste Management Radionuclide Report Series*, Idaho Falls, *Idaho*, 1995, vol. 17.

46 T. A. Marshall, K. Morris, G. T. W. Law, J. F. W. Mosselmans, P. Bots, H. Roberts and S. Shaw, *Mineral. Mag.*, 2015, **79**, 1265–1274.

47 J. R. Fox, R. J. G. Mortimer, G. Lear, J. R. Lloyd, I. Beadle and K. Morris, *Appl. Geochem.*, 2006, **21**, 1539–1550.

48 L. Newsome, K. Morris and J. R. Lloyd, *Chem. Geol.*, 2014, **363**, 164–184.

49 A. J. Williamson, K. Morris, G. T. W. Law, A. Rizoulis, J. M. Charnock and J. R. Lloyd, *Environ. Sci. Technol.*, 2014, **48**, 13549–13556.

50 H. Gamsjäger and F. J. Mompean, *Chem. Thermodyn.*, NEA Data Bank and OECD Nuclear Energy Agency, Issy-les-Moulineaux (France), 2005, p. 617.

51 G. Kuippers, C. Boothman, H. Bagshaw, M. Ward, R. Beard, N. Bryan and J. R. Lloyd, *Sci. Rep.*, 2018, **8**, 1–11.

52 G. Joshi-Tope and A. J. Francis, *J. Bacteriol.*, 1995, **177**, 1989–1993.

53 A. J. Francis, *J. Alloys Compd.*, 1998, **271–273**, 78–84.

54 A. J. Francis and C. J. Dodge, *Environ. Sci. Technol.*, 2008, **42**, 8277–8282.

55 Y. Suzuki, T. Nankawa, T. Yoshida, T. Ozaki, T. Ohnuki, A. J. Francis, S. Tsushima, Y. Enokida and I. Yamamoto, *J. Radioanal. Nucl. Chem.*, 2005, **266**(2), 199–204.

56 R. Ganesh, K. G. Robinson, L. Chu, D. Kucsmas and G. D. Reed, *Water Res.*, 1999, **33**, 3447–3458.

57 R. Ganesh, K. G. Robinson, G. D. Reed and G. S. Sayler, *Appl. Environ. Microbiol.*, 1997, **63**, 4385–4391.

58 F. Y. C. Huang, P. V. Brady, E. R. Lindgren and P. Guerra, *Environ. Sci. Technol.*, 1998, **32**, 379–382.

59 A. J. Francis, *Uranium Environ. Min. Impact Consequences*, 2006, 191–197.

60 A. J. Francis, G. A. Joshi-Tope and C. J. Dodge, *Environ. Sci. Technol.*, 1996, **30**, 562–569.

61 A. J. Francis and C. J. Dodge, *Appl. Environ. Microbiol.*, 1993, **59**, 109–113.

62 R. A. P. Thomas, A. J. Beswick, G. Basnakova, R. Moller and L. E. Macaskie, *J. Chem. Technol. Biotechnol.*, 2000, **75**, 187–195.

63 W. Hummel, G. Anderegg, I. Puigdomenech, R. Linfeng and O. Tochiyama, *Radiochim. Acta*, 2005, **93**, 719–725.

© 2023 The Author(s). Published by the Royal Society of Chemistry

Environ. Sci.: Adv., 2023, **2**, 1196–1209 | **1207**

64 E. Giffaut, M. Grivé, P. Blanc, P. Vieillard, E. Colàs, H. Gailhanou, S. Gaboreau, N. Marty, B. Madé and L. Duro, *Appl. Geochem.*, 2014, **49**, 225–236.

65 E. Colàs, M. Grivé, I. Rojo and L. Duro, *Radiochim. Acta*, 2011, **99**, 269–273.

66 E. Colàs, M. Grivé and I. Rojo, *J. Solution Chem.*, 2013, **42**, 1545–1557.

67 E. Colàs, M. Grivé, I. Rojo and L. Duro, *J. Solution Chem.*, 2013, **42**, 1680–1690.

68 K. Vercammen, M. A. Glaus and L. R. Van Loon, *Radiochim. Acta*, 2001, **89**, 393–401.

69 Z. A. Begum, I. M. M. Rahman, Y. Tate, Y. Egawa, T. Maki and H. Hasegawa, *J. Solution Chem.*, 2012, **41**, 1713–1728.

70 L. Abrahamsen-Mills and J. S. Small, *Organic-containing nuclear wastes and national inventories across Europe*, Elsevier Inc., 2021, vol. 2.

71 R. A. Peterson, E. C. Buck, J. Chun, R. C. Daniel, D. L. Herting, E. S. Ilton, G. J. Lumetta and S. B. Clark, *Environ. Sci. Technol.*, 2018, **52**, 381–396.

72 J. Small, C. Lennon and L. Abrahamsen, *GRM Near-Field Modelling for the LLWER 2011 ESC*, 2011, www.llwrsite.com, accessed 25 October 2017.

73 A. Rizoulis, H. M. Steele, K. Morris and J. R. Lloyd, *Mineral. Mag.*, 2012, **76**, 3261–3270.

74 S. L. Smith, A. Rizoulis, J. M. West and J. R. Lloyd, *Geomicrobiol. J.*, 2016, **33**, 455–467.

75 J. Qian, D. Li, G. Zhan, L. Zhang, W. Su and P. Gao, *Bioresour. Technol.*, 2012, **116**, 66–73.

76 J. Qian, X. Zhu, Y. Tao, Y. Zhou, X. He and D. Li, *Int. J. Mol. Sci.*, 2015, **16**, 7932–7943.

77 C. Robinson, M. White-Pettigrew, S. Shaw, K. Morris, J. Graham and J. R. Lloyd, *J. Nucl. Fuel Cycle Waste Technol.*, 2022, **20**, 307–319.

78 J. A. Schramke, E. F. U. Santillan and R. T. Peake, *Appl. Geochem.*, 2020, **116**, 104561.

79 E. Santillan, G. Chen, P. Flanders, H. Leigh, J. Major, D. Malashock, T. Peake, K. Reiser, J. Rustick, J. Schramke, D. Schultheisz, D. Stuenkel and X. Tong, *The Geochemistry of the Waste Isolation Pilot Plant*, 2021.

80 D. L. Wilson, M. L. Baker, B. R. Hart, J. E. Marra and P. E. Shoemaker, *Waste Isolation Pilot Plant Technical Assessment Team Report*, 2015.

81 D. L. Parkhurst and C. A. J. Appelo, *Description of input and examples for PHREEQC version 3-A computer program for speciation, batch-reaction, one-dimensional transport, and inverse geochemical calculations*, 2013, https://pubs.usgs.gov/tm/06/a43/, accessed 24 April 2020.

82 A. E. Milodowski, R. P. Shaw and D. I. Stewart, *British Geological Survey Commissioned Report*, CR/13/104 43pp, 2013.

83 D. R. Lovley, R. C. Greening and J. G. Ferry, *Appl. Environ. Microbiol.*, 1984, **48**, 81–87.

84 J. R. Postgate, *The sulphate-reducing bacteria*, Cambridge University Press, Cambridge, 2nd edn, 1984.

85 J. G. Caporaso, *Proc. Natl. Acad. Sci.*, 2011, 4516–4522.

86 J. G. Caporaso, C. L. Lauber, W. A. Walters, D. Berg-Lyons, J. Huntley, N. Fierer, S. M. Owens, J. Betley, L. Fraser, M. Bauer, N. Gormley, J. A. Gilbert, G. Smith and R. Knight, *ISME J.*, 2012, **6**, 1621–1624.

87 J. J. Kozich, S. L. Westcott, N. T. Baxter, S. K. Highlander and P. D. Schloss, *Appl. Environ. Microbiol.*, 2013, **79**, 5112–5120.

88 P. L. McCarty, *Biotechnol. Bioeng.*, 2006, **97**, 377–388.

89 G. R. Hedwig, J. R. Liddle and R. D. Reeves, *Aust. J. Chem.*, 1980, **33**, 1685–1693.

90 L. Macomber and R. P. Hausinger, in *Stress and Environmental Regulation ofGene Expression and Adaptation in Bacteria*, ed. F. J. de Bruijn, John Wiley & Sons Inc., First., 2016, pp. 1133–1141.

91 L. Macomber and R. P. Hausinger, *Metallomics*, 2011, **3**, 1153–1162.

92 N. V. Ashley, M. Davies and T. J. Hurst, *Water Res.*, 1982, **16**, 963–971.

93 Y. Suzuki and J. F. Banfield, *Geomicrobiol. J.*, 2004, **21**, 113–121.

94 M. P. Thorgersen, W. Andrew Lancaster, X. Ge, G. M. Zane, K. M. Wetmore, B. J. Vaccaro, F. L. Poole, A. D. Younkin, A. M. Deutschbauer, A. P. Arkin, J. D. Wall and M. W. W. Adams, *Front. Microbiol.*, 2017, **8**, 1–12.

95 C. Buchmaier, M. Glänzer, A. Torvisco, P. Poelt, K. Wewerka, B. Kunert, K. Gatterer, G. Trimmel and T. Rath, *J. Mater. Sci.*, 2017, **52**, 10898–10914.

96 G. Barim, S. R. Smock, P. D. Antunez, D. Glaser and R. L. Brutchey, *Nanoscale*, 2018, **10**, 16298–16306.

97 E. M. van den Berg, M. P. Elisário, J. G. Kuenen, R. Kleerebezem and M. C. M. van Loosdrecht, *Front. Microbiol.*, 2017, **8**, 1–13.

98 C. Allison and G. T. Macfarlane, *J. Gen. Microbiol.*, 1988, **134**, 1397–1405.

99 A. Hanke, J. Berg, T. Hargesheimer, H. E. Tegetmeyer, C. E. Sharp and M. Strous, *Front. Microbiol.*, 2016, **6**, 1461.

100 A. Chidthaisong and R. Conrad, *FEMS Microbiol. Ecol.*, 2000, **31**, 73–86.

101 J. R. Bargar, K. H. Williams, K. M. Campbell, P. E. Long, J. E. Stubbs, E. I. Suvorova, J. S. Lezama-Pacheco, D. S. Alessi, M. Stylo, S. M. Webb, J. A. Davis, D. E. Giammar, L. Y. Blue and R. Bernier-Latmani, *Proc. Natl. Acad. Sci. U. S. A.*, 2013, **110**, 4506–4511.

102 D. S. Alessi, J. S. Lezama-Pacheco, J. E. Stubbs, M. Janousch, J. R. Bargar, P. Persson and R. Bernier-Latmani, *Geochim. Cosmochim. Acta*, 2014, **131**, 115–127.

103 A. Bhattacharyya, K. M. Campbell, S. D. Kelly, Y. Roebbert, S. Weyer, R. Bernier-Latmani and T. Borch, *Nat. Commun.*, 2017, **8**, 1–8.

104 G. Kuippers, K. Morris, L. T. Townsend, P. Bots, K. Kvashnina, N. D. Bryan and J. R. Lloyd, *Environ. Sci. Technol.*, 2021, **55**(8), 4597–4606.

105 A. J. Fuller, P. Leary, N. D. Gray, H. S. Davies, J. F. W. Mosselmans, F. Cox, C. H. Robinson, J. K. Pittman, C. M. McCann, M. Muir, M. C. Graham, S. Utsunomiya, W. R. Bower, K. Morris, S. Shaw, P. Bots, F. R. Livens and G. T. W. Law, *Chemosphere*, 2020, **254**, 126859.

106 M. I. Boyanov, K. E. Fletcher, M. J. Kwon, X. Rui, E. J. O'Loughlin, F. E. Löffler and K. M. Kemner, *Environ. Sci. Technol.*, 2011, **45**, 8336–8344.

107 G. Morin, A. Mangeret, G. Othmane, L. Stetten, M. Seder-Colomina, J. Brest, G. Ona-Nguema, S. Bassot, C. Courbet, J. Guillevic, A. Thouvenot, O. Mathon, O. Proux and J. R. Bargar, *Geochemical Perspect. Lett.*, 2016, **2**, 95–105.

108 R. Bernier-Latmani, H. Veeramani, E. D. Vecchia, P. Junier, J. S. Lezama-Pacheco, E. I. Suvorova, J. O. Sharp, N. S. Wigginton and J. R. Bargar, *Environ. Sci. Technol.*, 2010, **44**, 9456–9462.

109 L. Newsome, K. Morris, D. Trivedi, A. Bewsher and J. R. Lloyd, *Environ. Sci. Technol.*, 2015, **49**, 11070–11078.

110 D. G. Zavarzina, T. P. Tourova, T. V. Kolganova, E. S. Boulygina and T. N. Zhilina, *Microbiology*, 2009, **78**, 723–731.

111 R. A. Albert, M. McGuine, S. C. Pavlons, J. Roecker, J. Bruess, S. Mossman, S. Sun, M. King, S. Hong, C. E. Farrance, J. Danner, Y. Joung, N. Shapiro, W. B. Whitman and H. J. Busse, *Int. J. Syst. Evol. Microbiol.*, 2019, **69**, 1376–1383.

112 A. K. Borsodi, J. M. Aszalós, P. Bihari, I. Nagy, P. Schumann, C. Spröer, A. L. Kovacs, K. Bóka, P. Dobosy, M. Óvari, T. Szili-Kovacs and E. Tóth, *Int. J. Syst. Evol. Microbiol.*, 2019, **69**, 631–637.

113 G. Hernandez-Eugenio, M. L. Fardeau, B. K. C. Patel, H. Macarie, J. L. Garcia and B. Ollivier, *Anaerobe*, 2000, **6**, 305–312.

114 E. V. Pikuta and R. B. Hoover, *Lact. Acid Bact. Biodivers. Taxon.*, 2014, **9781444333**, 135–145.

115 T. Černoušek, R. Shrestha, H. Kovářová, R. Špánek, A. Ševců, K. Sihelská, J. Kokinda, J. Stoulil and J. Steinová, *Corros. Eng., Sci. Technol.*, 2020, **55**, 127–137.

116 F. King, M. Kolar, S. Stroes-Gascoyne, P. Bellingham, J. Chu and P. V Dawe, *MRS Online Proc. Libr.*, 1999, **556**, 1167.

117 K. Pedersen, *J. Appl. Microbiol.*, 2010, **108**, 1094–1104.

118 M. Motamedi, O. Karland and K. Pedersen, *FEMS Microbiol. Lett.*, 1996, **141**, 83–87.